Z. Phys. C – Particles and Fields 44, 1–13 (1989)

Zeitschrift für Physik C Particles and Fields

Measurement of the average lifetime of B hadrons

TASSO Collaboration

W. Braunschweig, R. Gerhards, F.J. Kirschfink, H.-U. Martyn
I. Physikalisches Institut, RWTH, Aachen, Federal Republic of Germany[a]

B. Bock[1], H.M. Fischer, H. Hartmann, J. Hartmann, E. Hilger, A. Jocksch, R. Wedemeyer
Physikalisches Institut, Universität, Bonn, Federal Republic of Germany[a]

B. Foster, A.J. Martin, A.J. Sephton
H.H. Wills Physics Laboratory, University of Bristol, Bristol, UK[b]

F. Barreiro[2], E. Bernardi[3], J. Chwastowski[4], A. Eskreys[4], K. Gather, K. Genser[5], H. Hultschig, P. Joos, H. Kowalski, A. Ladage, B. Löhr, D. Lüke, P. Mättig[6], D. Notz, J.M. Pawlak[5], K.-U. Pösnecker, E. Ros, D. Trines, R. Walczak[5], G. Wolf
Deutsches Elektronen-Synchrotron DESY, Hamburg, Federal Republic of Germany

H. Kolanoski
Institut für Physik, Universität, Dortmund, Federal Republic of Germany[a]

T. Kracht[7], J. Krüger, E. Lohrmann, G. Poelz, W. Zeuner
II. Institut für Experimentalphysik, Universität, Hamburg, Federal Republic of Germany[a]

A. Belk, D.M. Binnie, J. Hassard, J. Shulman, D. Su[8]
Department of Physics, Imperial College, London, UK[b]

A. Leites, J. del Peso
Universidad Autonoma de Madrid, Madrid, Spain[c]

C. Balkwill, M.G. Bowler, P.N. Burrows[8], R.J. Cashmore, G.P. Heath, P.N. Ratoff, I.M. Silvester, I.R. Tomalin[9], M.E. Veitch
Department of Nuclear Physics, Oxford University, Oxford, UK[b]

G.E. Forden[10], J.C. Hart, D.H. Saxon
Rutherford Appleton Laboratory, Chilton, Didcot, UK[b]

S. Brandt, M. Holder, L. Labarga[11]
Fachbereich Physik, Universität-Gesamthochschule, Siegen, Federal Republic of Germany[a]

Y. Eisenberg, U. Karshon, G. Mikenberg, A. Montag, D. Revel, E. Ronat, A. Shapira, N. Wainer, G. Yekutieli
Weizmann Institute, Rehovot, Israel[d]

A. Caldwell[12], D. Muller, S. Ritz[12], D. Strom[13], M. Takashima, Sau Lan Wu, G. Zobernig
Department of Physics, University of Wisconsin, Madison, WI, USA[e]

Received 26 November 1988

[1] Now at Krupp Atlas Elektr. GmbH, Bremen, FRG
[2] Alexander v. Humboldt fellow, on leave from Universidad Autonoma de Madrid
[3] Now at Robert Bosch GmbH, Schwieberdingen, FRG
[4] Now at Inst. of Nuclear Physics, Cracow, Poland
[5] Now at Warsaw University[f], Poland
[6] Now at IPP Canada, Carleton University, Ottawa, Canada
[7] Now at Hasylab, DESY
[8] Now at RAL, Chilton, Didcot, UK
[9] Now at Imperial College, London, UK
[10] Now at SUNY Stony Brook, Stony Brook, NY, USA
[11] Now at SLAC, Stanford, CA, USA
[12] Now at Columbia University, NY, USA
[13] Now at University of Chicago, Chicago, IL, USA

Abstract. The average lifetime of B hadrons has been measured by the TASSO collaboration using 110 pb^{-1} of data collected in 1986 at a center of mass energy of 35 GeV. Measurements by three different

[a] Supported by Bundesministerium für Forschung und Technologie
[b] Supported by UK Science and Engineering Research Council
[c] Supported by CAICYT
[d] Supported by the Minerva Gesellschaft für Forschung GmbH
[e] Supported by US Dept. of Energy, contract DE-AC02-76ER000881 and by US Nat. Sci. Foundation Grant no INT-8313994 for travel
[f] Partially supported by grant CPBP 01.06

methods are presented and a method of B-enrichment is discussed. The result of the impact parameter method is $\tau_B = 1.36 \pm 0.13 \pm 0.28$ ps, that of the vertex method is $\tau_B = 1.30 \pm 0.10 \pm 0.28$ ps and that of the dipole method is $\tau_B = 1.47 \pm 0.14 \pm 0.30$ ps. These are combined to give the result $\tau_B = 1.35 \pm 0.10 \pm 0.24$ ps.

1 Introduction

In the Standard Model, a B hadron decays via a flavor changing transition which depends upon the weak mixing among different quark generations. This mixing has been expressed in matrix form for three quark generations by Kobayashi and Maskawa [1]. A measurement of the B hadron lifetime, τ_B, can then be used to constrain the relevant elements of this mixing matrix.

In 1982, the JADE collaboration presented the first upper limit for the average B hadron lifetime [2]. The MAC [3] and Mark II [4] collaborations followed with the first measurements of τ_B within the next year. Since then, six experiments at PEP and PETRA have published results on measurements of τ_B [5–7]. In this paper, we present our final determinations of τ_B using three different methods. These results are derived from data taken during the 1986 running period at the PETRA storage ring. A total integrated luminosity of 110 pb^{-1} was collected with the TASSO detector [8] at a center of mass energy of 35 GeV. We analyzed 31000 hadronic events with the aid of a high precision vertex detector, which is 16 times the amount of vertex detector data available for the previous TASSO publication [7]. The results presented here are statistically independent of the previous analysis since there are no data in common.

At PEP and PETRA energies, the full reconstruction of B hadrons has not been possible owing to the high average charged particle multiplicity of B hadron decays, the small branching ratios for individual low multiplicity channels, and the large number of fragmentation tracks prevalent in high energy events. The determination of τ_B has therefore relied on indirect techniques which infer the lifetime from a comparison of the data with Monte Carlo simulations. In this environment, it is only possible to measure the average lifetime of the combination of B hadron species in the data.

The indirect nature of B lifetime measurement prompts us to use three different methods, the "impact parameter method", the "vertex method", and the "dipole method", which have different sensitivities to systematic effects such as models of heavy quark fragmentation and B hadron decay. In the impact parameter method, the signed impact parameters of all selected tracks in an event are measured with respect to the estimated primary e^+e^- interaction point. The impact parameter technique has the advantage of being largely insensitive to the boost of the B hadron and therefore to the heavy quark fragmentation function. In the vertex method, the best three prong vertex in a jet is found and its distance from the primary interaction point is measured. Because of the high average energy and charged decay multiplicity of B hadrons, this vertex is a strong candidate for an actual B hadron decay point. In the dipole method, we measure the "dipole moment" which is the separation between the estimated decay vertices in the two opposite jets in an event. A measurement of the dipole moment is independent of the errors involved in estimating the primary interaction point. These three methods will be described in detail in Sects. 3–5 of this paper. A description of the Monte Carlo simulation used to extract the lifetimes and a discussion of the associated systematic errors will be presented in Sect. 6.

B hadrons are present in only 1/11 of continuum e^+e^- hadronic annihilation events. Therefore in one method, the impact parameter method, we reduce the statistical background of other flavors by an enrichment technique based on an event shape parameter to be described in Sect. 2. This method relies only on the larger average sphericities of B hadron jets compared to those from lighter flavors and is thus unbiased with respect to the particle lifetime. In the other two methods, this enrichment technique is not necessary for the lifetime measurement, but has been applied in the study of systematic effects. All three methods are somewhat different from those published by other experiments. In particular, other published methods include enrichment techniques based on isolated high transverse momentum leptons from semileptonic B hadron decays. These methods are sensitive to the B hadron semileptonic branching ratios and may preferentially select the B hadrons with longer lifetimes.

2 The boosted sphericity product method for $b\bar{b}$ event enrichment

Lifetime measurements of B hadrons are sofar the exclusive domain of higher energy e^+e^- experiments. However, since a b quark has charge $-1/3$, only 1/11 of continuum hadronic events contain B hadrons. It is desirable to suppress the background from lighter flavors and, in particular, charm quark events which contribute long-lived final state hadrons such as D^0 and D^+ mesons. The relative enrichment of the data sample with $b\bar{b}$ events then may improve the statisti-

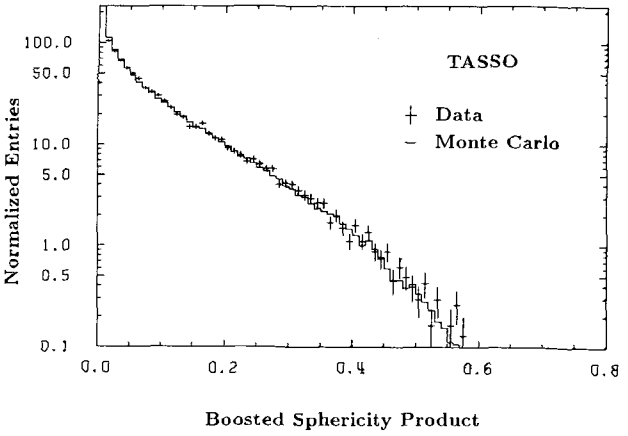

Fig. 1. Distribution of the boosted sphericity product, $S_1 S_2$. The crosses represent the data while the Monte Carlo simulation is displayed with the solid line histogram

Table 1. The fractions of data and Monte Carlo events for which $S_1 S_2$ is greater than the given cut are shown with the corresponding B purity. The errors are statistical only

$S_1 S_2 \geqq$	Data fraction (%)	Monte Carlo fraction (%)	B purity (%)
0.02	66.6±0.4	67.5±0.1	13.7±0.1
0.04	51.7±0.5	51.5±0.2	16.3±0.2
0.06	41.0±0.5	40.9±0.2	18.6±0.2
0.08	32.7±0.4	33.1±0.1	20.6±0.2
0.10	26.7±0.4	27.0±0.1	22.7±0.2
0.12	21.8±0.4	22.0±0.1	24.7±0.3
0.14	18.2±0.4	18.0±0.1	26.8±0.3
0.16	15.0±0.3	14.9±0.1	28.3±0.4
0.18	12.2±0.3	12.2±0.1	29.9±0.4
0.20	10.0±0.3	9.9±0.1	31.4±0.5
0.22	8.3±0.3	8.1±0.1	33.3±0.5
0.24	7.0±0.2	6.6±0.1	35.0±0.6

cal significance of lifetime measurements and also provides an opportunity to study the reliability of the Monte Carlo simulation.

We enrich the data sample with $b\bar{b}$ events through the use of an event shape parameter called the 'boosted sphericity product' [7] or '$S_1 S_2$'. This enrichment scheme utilizes the higher average sphericity of b quark jets to separate events with B hadrons from those which contain lighter primary quarks. The high jet sphericities are a consequence of the large rest mass (5.28 GeV [9]) of the B hadrons. The separation of flavors can be further enhanced if the jet sphericities are measured in a Lorentz frame which is a result of a boost toward the B hadron rest frame. The $S_1 S_2$ parameter is constructed by multiplying the two boosted jet sphericities, S_1 and S_2 in each two-jet event.

The $S_1 S_2$ parameter is calculated from tracks which are reconstructed in the central drift chamber [10]. The events must be well contained in the detector to ensure reliable sphericity measurements. Therefore, the modulus of the cosine of the angle between the sphericity axis and the beam is restricted to be less than 0.7. Since the enrichment is based on the relative sphericities of the different quark flavors, three-jet events, which possess high average sphericity and thus constitute background events, must be taken into account. Three-jet event candidates are selected using a three-jet finding algorithm [11] and then removed from the data sample. In order for an event to be positively identified as a three-jet event, it must meet the following criteria: *i)* the sphericity of the event must be greater than 0.2; *ii)* each of the three jets must have at least 2 charged tracks; *iii)* each of the three jets must have a reconstructed energy greater than 2 GeV (assuming the mass of a pion); *iv)* the minimum angle between any two jet axes must be greater than 45 degrees. After these cuts, ~10% of the events, in both the data and the Monte Carlo simulation, are classified as three-jet events.

The remaining events are divided into two jets defined by the plane perpendicular to the sphericity axis. The two jets are boosted along the direction of the sphericity axis towards their hypothetical B hadron rest frames. The β value for the boost is tuned, from the Monte Carlo simulation (the QCDFF Monte Carlo simulation used for these studies is described in detail in Sect. 6), to 0.74 to optimize the separation of $b\bar{b}$ events from $c\bar{c}$ events at $\sqrt{s}$ = 35 GeV. The sphericities of both jets are calculated independently in the respective boosted frames and are multiplied to form the enrichment parameter $S_1 S_2$. In Fig. 1 the $S_1 S_2$ distributions are shown for both the data (points with error bars) and the Monte Carlo simulation.

The data can be studied in different regions of the $S_1 S_2$ distribution by placing cuts at given $S_1 S_2$ values. The property of most interest is how the fraction of $b\bar{b}$ events in the data samples varies as a function of the cut value. The relative fractions can be extracted by applying cuts to the $S_1 S_2$ distributions from the data and comparing with the Monte Carlo simulation. Therefore, in order to determine this fraction reliably, the relative numbers of Monte Carlo and data events passing a certain cut must be in agreement. Table 1 displays the fraction of all events which pass a given cut in the data and Monte Carlo simulations and also shows the "B purity", the fraction of $b\bar{b}$ events in the Monte Carlo data sample as a function of these cuts. We define a 'B enriched' region, or a region where the data sample is enriched with $b\bar{b}$ events, by requiring that events have $S_1 S_2 \geqq 0.18$.

The percentage of all events which pass this cut is $12.2 \pm 0.3\%$ for the data compared with $12.2 \pm 0.1\%$ for the Monte Carlo simulation, where the errors are statistical only. The B enriched region consists of 30% primary $b\bar{b}$ events, 31% primary $c\bar{c}$ events, and 39% primary $u, d,$ and s events. Approximately 36% of $b\bar{b}$ events pass the enrichment cut. A region depleted in $b\bar{b}$ events can also be defined by requiring $S_1 S_2 \leq 0.02$. In this region, $b\bar{b}$ events comprise only 2.5% of the event sample. Note that this enrichment scheme uses only charged tracks, and we would expect a higher $b\bar{b}$ fraction in the enriched sample if we could include neutral particles.

The $S_1 S_2$ variable can also be incorporated into a weighting scheme, as proposed by the JADE collaboration [12], to enrich the data sample instead of using a simple cut. In this procedure, a global weight is assigned to an event, based on the probability that it is a $b\bar{b}$ event. The $S_1 S_2$ parameter is used as a discriminator variable to calculate the event weight. By using this weighting technique all hadronic events are considered, and therefore all $b\bar{b}$ events are retained, resulting in a higher statistical significance. $S_1 S_2$ distributions are generated by Monte Carlo simulations for both 'signal' b quark events and 'background' $u, d, s,$ and c quark events. From these two distributions, a weight function is constructed such that the variance of the sum of these weights is minimized. If x is taken to be the discriminator variable, the optimal weight function is written:

$$w(x) = \frac{s(x)}{s(x) + A \cdot b(x)} \tag{1}$$

where $s(x)$ and $b(x)$ are the signal and background distributions normalized to unity and A is the ratio of background to signal events.

3 The impact parameter method

In this method, signed impact parameters of all selected charged tracks in events from a B enriched data sample are used to measure τ_B. The selection criteria are described below. Because of their large average boost and decay multiplicity, B hadrons contribute most of the high momentum tracks in $b\bar{b}$ events. Hence, using all such tracks in an event increases the sensitivity of the lifetime measurement to B hadron decays relative to decays of primary hadrons from lighter flavor events.

The impact parameter is defined as the distance of closest approach of a track to the estimated primary interaction point. We measure this variable in the $r-\phi$ projection, the plane perpendicular to the beam axis, because of the much better spatial and momentum resolutions in this plane compared to those in the z direction. In addition, the beam bunch size is much more restricted in the $r-\phi$ projection than along the beam axis. Figure 2a shows the definition of the impact parameter in the $r-\phi$ projection. In order to attribute a sign to the impact parameter, the B hadron flight path is assumed to follow the direction of the sphericity axis from the center of the beam spot into the hemisphere containing the track. A track's impact parameter is given a sign depending on where the track crosses the sphericity axis in relation to the position of the primary interaction point in the $r-\phi$ projection. An impact parameter obtains a positive sign if the crossing point of the track with the sphericity axis corresponds to a positive decay time of the assumed B hadron (see Fig. 2b).

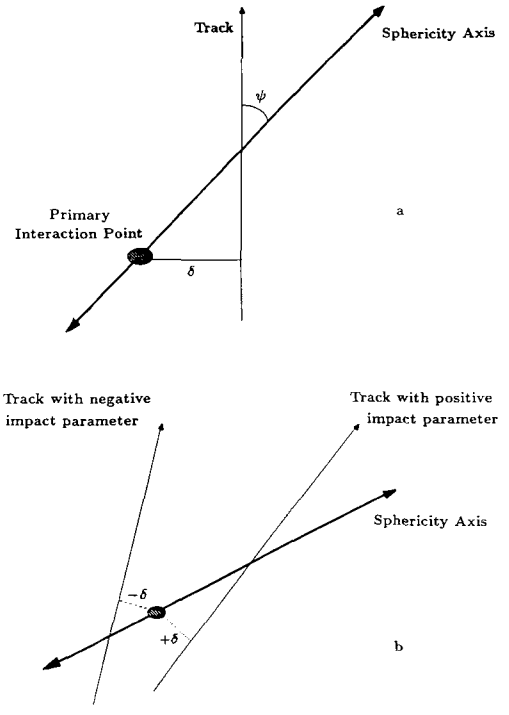

Fig. 2. a Definition of the impact parameter. **b** The sign is positive if the crossing point of the track with the sphericity axis corresponds to a positive decay time of the assumed B hadron

The impact parameter of a track which originates from an isotropic decay of a high energy particle has the advantage of being largely independent of the particle's momentum. From Fig. 2a, the impact parameter is defined in the $r-\phi$ projection as

$$\delta = \gamma\beta \cdot c\tau \cdot \sin\psi \cdot \sin\theta, \tag{2}$$

where ψ is the angle between the decay track and the direction of flight of the decaying particle in $r-\phi$, θ is the polar angle of the track with respect to the beam, and τ is the proper decay time. For

highly relativistic particles, $\langle \sin\psi \rangle \sim 1/\gamma\beta$ and the mean impact parameter depends only on $\langle c\tau \rangle$.

Tracks which originate from decays of long lived particles, such as B hadrons, contribute large positive impact parameters compared to tracks from short lived hadronic decays and primary fragmentation. The average B hadron lifetime is then determined by measuring the positive shift in the impact parameter distribution and comparing this value to Monte Carlo simulations which are generated with different values of τ_B.

The lifetime measurement using the impact parameter method requires that the primary interaction vertex be reliably estimated. This vertex lies within the overlap region of the electron and positron beams (beam spot). Because the size of this interaction region is extended over several centimeters in z and due to the relatively poor tracking information in this coordinate, the determination of the beam spot is restricted to the $r-\phi$ projection. The beam spot position was found to be rather sensitive to changes in the operation of PETRA, so we measured its position on a fill-by-fill basis, averaging sequential fills only when insufficient data existed from a single filling of the storage ring.

The details of the beam spot calculation can be found in [13]. We repeat the important features here. The beam spot is calculated from selected beam-associated tracks which are reconstructed in both the vertex chamber and the central drift chamber. A minimum of 50 tracks per fill is required for an accurate determination. A χ^2 for each track is defined as follows:

$$\chi_i^2 = \frac{\delta_i^2}{\sigma_\delta^2} + \frac{(x_i - x_b)^2}{\sigma_x^2} + \frac{(y_i - y_b)^2}{\sigma_y^2}, \tag{3}$$

where δ_i is the impact parameter of the track with respect to the hypothesized interaction point (x_i, y_i) for an event and (x_b, y_b) is the most likely center of the beam spot. The sizes σ_x and σ_y are estimated to be 500 μm and 60 μm respectively. The calculated beam spots are not found to be sensitive to changes in these sizes. The term σ_δ is the sum in quadrature of the intrinsic detector impact parameter resolution and a multiple scattering term, which is inversely proportional to the momentum of the track. By minimizing the χ_i^2 of each track with respect to (x_i, y_i), the χ_i^2 can be expressed such that only the coordinates of the most likely center of the beam spot, (x_b, y_b) remain as free parameters. During the χ^2 minimization procedure, the terms σ_x, σ_y, and σ_δ are held fixed to their input values. A global χ^2 for a fill can be defined by summing the individual track χ_i^2 in the fill. This expression is then minimized to extract (x_b, y_b) along with their errors.

Having obtained the beam positions, we use a data sample of clean two track events to make an accurate measurement of the *rms* sizes of the interaction region, σ_x and σ_y, which includes possible effects due to beam movement. We measure the width of the distribution of impact parameters with respect to (x_b, y_b) as a function of the azimuth, ϕ_0, of a track's momentum vector at its point of closest approach to the center of the detector coordinate system. The size of the interaction region is found to vary between 300 μm and 520 μm in x, and 60 μm and 120 μm in y, depending on the beam energy and stability of its position. The two-dimensional errors on the primary interaction point are taken as the measured beam spot size added in quadrature with the statistical errors on the determination of the center of the beam spot.

In using the impact parameter method, we apply the S_1S_2 weighting method which is described in the previous section. Tracks which are reconstructed [14] from both the central drift chamber and the vertex chamber are refitted [15], including the effects of multiple scattering and the ability to delete hits to improve the fit χ^2. Tracks for the lifetime analysis are selected from this sample of refitted tracks according to the following criteria: *i)* the track momentum must be greater than 0.8 GeV; *ii)* the track must have at least 5 (of 8) layers of the vertex chamber recording a hit; *iii)* the χ^2 in $r-\phi$ of the fit must be $\leqq 5$ per degree of freedom; *iv)* the χ^2 in $s-z \leqq 20$ per degree of freedom (information in the z direction is included in the track finding by reconstructing charged tracks in the $s-z$ plane, for details see [10]), *v)* the distance in z from the center of the detector to the point of closest approach in $r-\phi$, z_0, must be $\leqq 3$ cm; *vi)* the track must cross the sphericity axis in the $r-\phi$ projection, *vii)* the impact parameter must be $\leqq 0.5$ cm; and *viii)* the angle between the track and the sphericity axis must be greater than $0.2/\sin\theta_s$ where θ_s is the polar angle of the sphericity axis to the beam direction. Criterion *vii* is chosen to reduce the effects of K_S^0 and Λ decays, while criterion *viii* reduces the incidence of impact parameter sign errors resulting from uncertainties in the sphericity axis direction.

Tracks meeting these requirements are weighted by the inverse square of the error on the impact parameter calculated from the covariance matrix determined by the track refitter. The average error on the impact parameter of a refit track which passes the selection criteria is ~ 180 μm. The resulting mean impact parameter from the data is 96.7 ± 5.0 μm. This mean is compared to those resulting from Monte Carlo simulations with different values of τ_B. The Monte Carlo simulated data is generated with a mean lifetime $\tau_B^0 = 2.0$ ps. The probability density for a distribu-

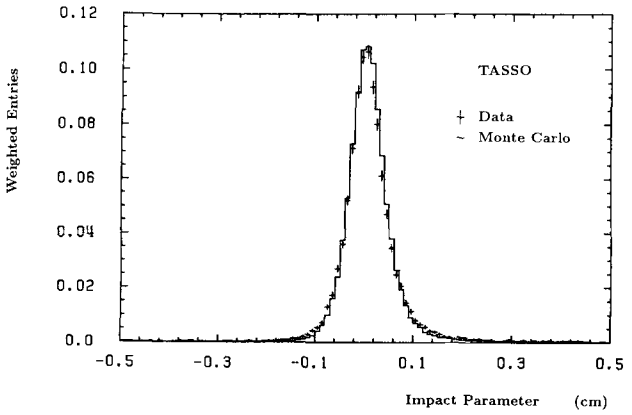

Fig. 3. Distribution of impact parameters for all selected tracks in the B-enriched data sample. The solid line is a Monte Carlo distribution with $\tau_B = 1.36$ ps and has the same mean

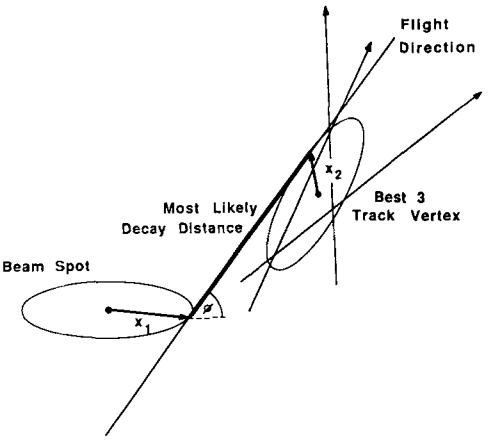

Fig. 4. Illustration of the vertex method. The best three prong vertex in a jet is found, and the most likely decay distance from the beam spot is calculated, using the sphericity axis as an estimate of the flight direction of the B hadron, as described in Sect. 4.

tion with mean lifetime τ_B^i is

$$P(t;\tau_B^i)\,dt = \frac{1}{\tau_B^i}\exp(-t/\tau_B^i)\,dt \tag{4}$$

where t is the proper time. In order to produce simulations with other lifetimes, the events in the Monte Carlo simulated sample are transformed from a distribution with mean lifetime τ_B^0 to one of τ_B^i by assigning a weight to each B hadron decay. This weight is a ratio of exponential decay distributions

$$W(t,\tau_B^0,\tau_B^i) = \left(\frac{\tau_B^0}{\tau_B^i}\right)\exp\left(-t\cdot\frac{\tau_B^0-\tau_B^i}{\tau_B^0\,\tau_B^i}\right). \tag{5}$$

The lifetime in the data is determined from the Monte Carlo simulation which gives the best agreement in the mean. This procedure yields an average B hadron lifetime of

$$\tau_B = (1.36 \pm 0.13)\ \text{ps},$$

where the error is statistical only. The simulation which gives the best agreement contributes means of 19.5 ± 2.4 μm from primary u, d, s events, 61.3 ± 2.8 μm from primary $c\bar{c}$ events and 294.5 ± 5.0 μm from primary $b\bar{b}$ events. Figure 3 shows the impact parameter distribution of the data as points with error bars, with the Monte Carlo simulation which gives the best agreement in the mean overlaid as the solid line histogram.

The vertex method

The second method used to measure the average B hadron lifetime is to search for decay vertices of B hadrons, and to measure their distances from the primary interaction point. We have not been able to reconstruct B hadrons, but their high average decay multiplicity and energy can be exploited by looking for several tracks which form a vertex distinct from the primary interaction point. By demanding vertices of very high quality, this method is sensitive to the presence of a long-lived particle with high decay multiplicity. We choose to seek a specific type of high quality vertex, the 'best' three-prong vertex, in each hemisphere of all two-jet events. The procedure is carried out in the $r-\phi$ projection and is illustrated in Fig. 4. No explicit scheme to enrich the data sample with $b\bar{b}$ events was used for this determination of τ_B.

Charged tracks are found [14] using both the central drift chamber and vertex detector and are required to *i)* be well reconstructed in three dimensions, *ii)* have hits in at least 5 (of 8) layers of the vertex detector, *iii)* have $z_0 < 3$ cm, and *iv)* pass a momentum cut of $p > 0.6$ GeV/c. The last cut reduces the effects of multiple scattering in the beam pipe, and preferentially selects tracks from leading particles, including B hadrons. After these cuts an average of 5.2 tracks remain per event.

Events are divided into two jets by the plane perpendicular to the sphericity axis. All combinations of three tracks in a single jet with total charge ± 1 are refitted in the $r-\phi$ projection with the addition of a constraint that they come from a common vertex [15]. The combination in each jet with the best vertex fit is accepted if the confidence level of the fit is greater than one percent. Since B hadrons have high average energy and charged decay multiplicity, they provide most of the selected tracks in b jets. This procedure therefore finds vertices near the B hadron decay point in these jets. Monte Carlo studies show that an average of 2.3 of the three tracks in vertices found in

b jets are from B decay products. The requirement of three tracks eliminates vertices from long lived neutrals, such as K_S^0 and Λ, and suppresses the contribution from charmed particles. In u, d and s quark jets, the vertices found are therefore near the primary interaction point. In c quark jets, the average D hadron has 55% of the beam energy and its decay produces 2.4 charged particles, of which only 1.3 are accepted. The method is therefore strongly biased against finding the decay vertex from a long lived charmed hadron and the selected vertices in c jets, which contain an average of 1.4 tracks from D decay products, are pulled toward the primary interaction point. A good vertex is found in 34% of all jets. There is a slight enhancement in the efficiency for b jets due to their higher multiplicity: about 12% of the vertices in selected events are in b jets.

The beam spot (see Sect. 3) is taken as an estimate of the production point of the decaying particle and the sphericity axis as an estimate of its flight direction. This flight direction measurement is reliable because three-jet events and events not well contained in the detector are removed as described in Sect. 2. The average angle in the $r-\phi$ projection between the sphericity axis and the actual $B(D)$ hadron momentum in Monte Carlo $b\bar{b}(c\bar{c})$ events is 140 (170 mrad. The most likely decay distance from the beam spot to the fitted vertex is computed by minimizing

$$\chi^2 = \mathbf{x}_1\, \sigma_B^{-1}\, \mathbf{x}_1 + \mathbf{x}_2\, \sigma_V^{-1}\, \mathbf{x}_2 + \frac{(\phi_p - \phi_S)^2}{(\Delta\phi)^2} \tag{6}$$

with respect to $\mathbf{x}_1$, $\mathbf{x}_2$, and ϕ_p. Here, $\sigma_{V(B)}$ is the vertex (primary interaction point) error matrix, $\mathbf{x}_{1(2)}$ is a vector from the primary interaction point (vertex) to the hypothesized production (decay) point of the particle. The third term in (6) is included to account for possible errors when estimating the decaying particle's flight path with the sphericity axis direction. In this term, ϕ_p is the azimuth of the particle flight path, and ϕ_S the azimuth of the sphericity axis, taken to point in the direction of the tracks in the jet (see Fig. 4). The accuracy of the sphericity axis as a measure of the flight direction, $\Delta\phi$, is the determined from Monte Carlo simulation to be 110 mrad. The measurement is rejected if this χ^2 corresponds to a confidence level of less than one percent, or if the calculated error on the decay distance is greater than 0.1 cm. These cuts remove events with a poorly determined sphericity axis.

Vertices are weighted by the inverse of the major axis of the vertex error ellipse. The distribution of the 13267 decay distances measured in the data is shown in Fig. 5 as the points with error bars. The mean of this distribution is 104 ± 9 μm.

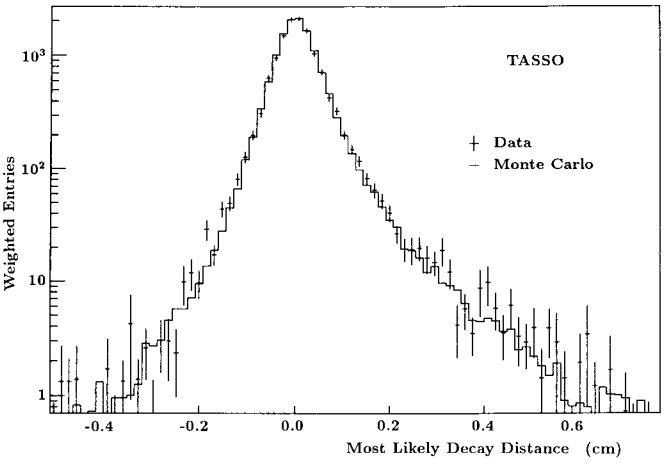

Fig. 5. Distribution of most likely decay distances. The points with error bars are the data. The solid line is a Monte Carlo distribution with $\tau_B = 1.30$ ps which gives the best fit to the data

This distribution is fitted to a normalized simulated distribution using a binned χ^2:

$$\chi^2 = \sum_i \frac{(N_i^{\text{data}} - N_i^{\text{sim}})^2}{(E_i^{\text{data}})^2 + (E_i^{\text{sim}})^2} \tag{7}$$

where the sum is over histogram bins, N_i is the sum of weights of entries in the i^{th} bin, and E_i is the error on that sum. At least eight data and eight Monte Carlo entries are required per bin and bins are combined until this number is reached. This χ^2 is minimized with respect to the B lifetime assumed in the Monte Carlo simulation using Monte Carlo histograms weighted to differerent B lifetimes as described in Sect. 3. The Monte Carlo distribution which best fits the data is the solid line in Fig. 5. Agreement between the two distributions is very good over three orders of magnitude, in particular on the negative side, which demonstrates a good understanding of the detector resolution. The minimum binned χ^2 is 77.5 for 52 degrees of freedom. The lifetime given by the fit is

$$\tau_B = 1.30 \pm 0.10 \text{ ps}$$

where the error is statistical only and corresponds to an increase of one in the binned χ^2. In the Monte Carlo simulated data sample, the mean decay distance is 9 μm for $u\bar{u}, d\bar{d}$ and $s\bar{s}$ events, 85 μm for $c\bar{c}$ events, and 550 μm for $b\bar{b}$ events generated with this lifetime.

5 The dipole method

The third method used to measure the average B lifetime constructs the dipole moment, ρ, which is a measure of the separation between vertices in opposite jets of an event. This method takes advantage of the

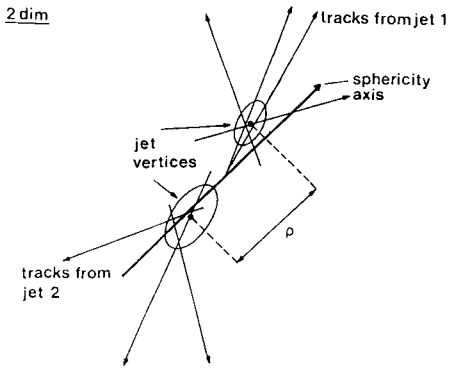

Fig. 6. Illustration of the dipole moment, ρ, A vertex is found in each jet of an event, and the distance between them is calculated as described in Sect. 5

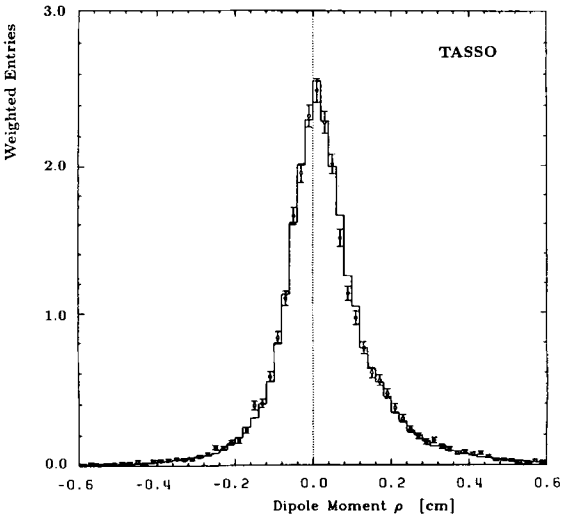

Fig. 7. Distribution of dipole moments. The points with error bars are the data and the solid line is a Monte Carlo distribution with $\tau_B = 1.50$ ps. A bin by bin comparison of the two distributions gives a total χ^2 of 70.6 for 60 bins

fact that two B hadrons are produced in nearly opposite directions in $b\bar{b}$ events and is sensitive to the sum of the two flight distances. This method also has the advantage that no measurement of the primary interaction point is needed. The dipole moment is computed in the $r-\phi$ projection and the procedure is illustrated in Fig. 6. As in the vertex method, no explicit scheme is used to enrich the data sample with $b\bar{b}$ events.

Events are required to be well contained in the detector and to have sphericity less than 0.35 to reduce the three-jet background. To ensure adequate statistics, the criteria for track and vertex selection are relaxed compared to the vertex method: charged tracks are found [14] using both the central drift chamber and vertex detector and are refitted in $r-\phi$ [15]. They are then required to *i)* be well reconstructed in three dimensions, *ii)* have $z_0 < 5$ cm, *iii)* have momentum in the $r-\phi$ plane $p_\perp > 0.2$ GeV/c, and *iv)* pass within 3 mm of the beam spot or cross the sphericity axis within 9 mm of the beam spot in the $r-\phi$ plane. An average of 8.3 tracks per event survive these cuts. These tracks have an average of 6.3 associated hits in the vertex detector. There must be at least three selected tracks in an event and at least one in each hemisphere.

In the $r-\phi$ projection, the sphericity axis is taken as an estimate of the flight directions of the two B hadrons. An event axis is defined by translating the projection of the sphericity axis to minimize the variance of the crossing points of the tracks in the event with this axis. In calculating this variance, tracks are weighted by $\sin^2\alpha$, where α is the crossing angle between the track and the event axis. The event is rejected if the event axis is more than 5 mm from the beam spot.

The event is divided into two jets by the plane perpendicular to the event axis. For each jet a vertex is found on the event axis by taking the average of the crossing points of the tracks in that jet with the axis. In computing this average, each track is weighted by its rapidity as well as by $\sin^2\alpha$. The dipole moment is the distance between these two vertices. It is given a negative sign if it corresponds to negative decay lengths.

The combination of rapidity and $\sin^2\alpha$ weights reduces the sensitivity of this method to variations of the heavy quark fragmentation and enhances the contribution from tracks coming from first rank fragmentation particles such as B hadrons. Since a majority of the tracks in $b\bar{b}$ events are from B hadron decays, the vertices are well separated and ρ is large in these events. In $u\bar{u}$, $d\bar{d}$ and $s\bar{s}$ events, however, both vertices are near the primary interaction point, and in $c\bar{c}$ events the vertices are pulled toward the primary interaction point because the majority of tracks in these events are from fragmentation rather than from decay products of the charmed hadrons.

Figure 7 shows the distribution of the 19143 measured dipole moments in the data weighted by their calculated errors. The mean value is $\langle\rho\rangle = 305 \pm 13$ μm. Model calculations show a contribution of 72 μm from beampipe scattering, K^0_S and Λ decays and 103 μm from charmed hadrons. The remaining 130 μm are assigned to bottom hadrons. The B lifetime is determined by a comparison of the mean of the data distribution with those of Monte Carlo simulations generated with different lifetimes. Figure 8 shows the mean dipole moment in the Monte Carlo as a function of the B lifetime used in the gener-

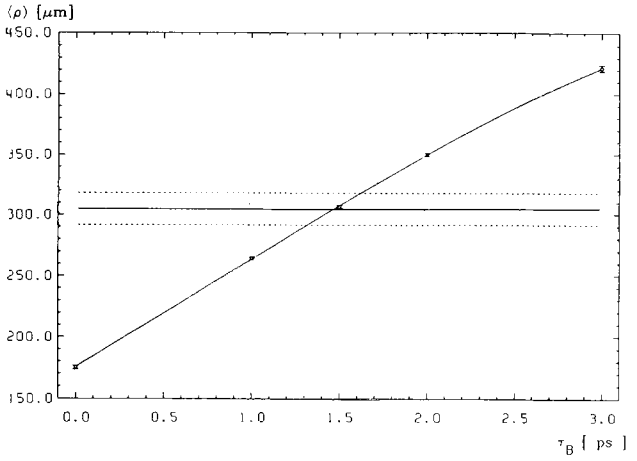

Fig. 8. Mean of the simulated dipole moment distribution vs. assumed B lifetime. The horizontal lines show the mean of the data and the one standard deviation errors

ation. The result of this comparison is

$\tau_B = 1.47 \pm 0.14$ ps

where the error is statistical only. The solid line in Fig. 7 is the Monte Carlo distribution for $\tau_b = 1.5$ ps. Monte Carlo u, d and s events have an average dipole moment of 70 μm, $c\bar{c}$ events have 320 μm and $b\bar{b}$ events with B lifetime 1.5 ps have 1040 μm. About 9% of the sample is $b\bar{b}$ events and these contribute about 15% of the total weight.

6 Systematic errors

In this section the dominant sources of systematic error in these measurements are discussed. These sources are common to the three methods, but affect them in different ways. Since the light quark background in the samples is large, it is important to understand the fraction of each sample due to events of each flavor. It is also important to know the mean of each distribution for events of each flavor. These depend on characteristics of the quark fragmentation process, the decay of heavy hadrons, and the detector resolution and acceptance which must be modelled.

6.1 Monte Carlo modelling

The Monte Carlo simulation which is used for the analysis procedure must incorporate all that is known about the production and decay of B hadrons to minimize systematic biases. In addition, relevant parameters should be easily adjustable over ranges which reflect the uncertainty in the knowledge entered into the simulation. The following models are therefore chosen to generate simulated events by Monte Carlo methods. Partons are generated according to second order QCD with extended FKSS [16] calculations. An independent jet fragmentation model is used with a Peterson [17] fragmentation function for heavy quarks. The average $z \equiv (E + p_{\parallel})_{\text{hadron}}/(E + |p|)_{\text{quark}}$ is set to $\langle z \rangle_{b(c)} = 0.81\ (0.67)$ for $b(c)$ quarks as suggested in recent reviews [18]. The width of the transverse fragmentation function has been set to $\sigma_q = 350$ MeV. This simulation has been developed over several years to match the event shapes of the TASSO data [19]. B hadron decay is simulated by a routine based on the jet model of [20] and tuned to CLEO data [21]. In particular the mean charged decay multiplicity of 5.50 (3.80 in semi-leptonic decays) and charged energy fraction of 0.627 are reproduced. We denote this simulation as the QCDFF Monte Carlo. The events are passed through a detailed simulation of the TASSO detector and then through the same event reduction, track finding and analysis routines as are the data.

In addition, the Lund [22] Monte Carlo version 6.2, incorporating the string model of fragmentation, has been used for systematic studies. This Monte Carlo has been tuned to the event shapes of the TASSO data at 35 GeV. However, the B decays from the Lund program do not reproduce the data on charged decay products measured by CLEO. Nor does this Monte Carlo model reproduce the distributions of charged track multiplicity and $S_1 S_2$ well enough for this analysis. Therefore this Monte Carlo model is not used for $b\bar{b}$ event simulation, but Lund light quark events are used for systematic studies of the lighter flavor background.

6.2 The average heavy hadron boosts

The flight distance of a particle of a given proper decay time is determined by its boost in the detector frame. The distribution of these boosts is determined by the fragmentation process, and can be parametrized by the quantity $\langle z \rangle$. The $\langle z \rangle$ values given above are varied in the Monte Carlo simulation by ± 0.05 to estimate the effect of uncertainty in these values. Errors on the measured lifetime of $\delta\tau_B = {}^{+0.09}_{-0.15}$ and $^{+0.11}_{+0.13}$ ps are thus estimated, for the impact parameter (IP), vertex (VX) and dipole (DM) methods respectively, due to uncertainty in $\langle z \rangle_b$. Variation of $\langle z \rangle_c$ gives error estimates of $\delta\tau_B = {}^{+0.04}_{-0.04}$ (IP), $^{+0.06}_{-0.06}$ (VX) and $^{+0.05}_{-0.05}$ (DM) ps for the three methods respectively.

6.3 The charmed particle lifetimes

The background in our samples from $c\bar{c}$ events has a positive average measured lifetime due to the rela-

tively long lifetimes of the charmed hadrons. In addition, the lifetimes of charmed particles from B hadron decays can affect the measured lifetime of the $b\bar{b}$ sample. These effects depend on the various lifetimes and relative abundances of the charmed hadrons. The following lifetimes are used [23]: $\tau_{D^0} = 0.429^{+0.012}_{-0.011}$ ps, $\tau_{D^+} = 1.029^{+0.035}_{-0.029}$ ps, $\tau_{D_s} = 0.433^{+0.041}_{-0.032}$ ps, $\tau_{\Lambda_c} = 0.164^{+0.024}_{-0.018}$ ps. The relative abundances are determined by the parameters:

Parameter	Central value	Range
Primary baryon production	10%	±2%
Primary strange quark production	$s/u = 0.4$	$0.3 < s/u < 0.5$
Pseudoscalar: vector production ratio	$p/v = 0.74$	$0.0 < p/v < 1.0$
BR $(D^{*+} \to D^0 X)$	55%	±8%

All charmed baryons are assumed to have the Λ_c lifetime. To estimate the error due to uncertainty in the charm lifetimes taking all possible correlations into account, the above lifetimes are varied together over their error ranges and the change in the measured B lifetime noted. The relative abundances of pseudoscalar charmed hadrons are then adjusted, in both simulated $c\bar{c}$ events and B hadron decays, to give the maximum and minimum average lifetimes allowed by the combined ranges of the lower four parameters. These two changes are added in quadrature to give estimates of the error due to the average charmed hadron lifetime of $\delta\tau_B = \mp 0.05$ (IP), ∓ 0.09 (VX) and ∓ 0.08 (DM) ps for the three methods.

6.4 *Flavor fractions*

The quark fragmentation and B hadron decay models also affect the measured τ_B indirectly. They affect the relative efficiencies of event, track or vertex selection for different flavors, and especially the $S_1 S_2$ B-enrichment scheme. The effect of uncertainty in the charged decay multiplicity of the B hadrons is evaluated by varying the multiplicity over the range $5.30 < \langle N_{ch} \rangle < 5.70$, resulting in $\delta\tau_B = \pm 0.05$ (IP), ± 0.05 (VX) and ± 0.06 (DM) ps. We have done several consistency checks to put limits on additional uncertainties in the model.

A good check on the $b\bar{b}$ fraction of the samples and on the consistency of the $S_1 S_2$ enrichment scheme is to investigate the measured lifetime in a large number of different ranges of $S_1 S_2$ and for a variety of different weighting functions. The IP and VX methods have been checked in this way and variations of the measured lifetimes are less than 15%. The B-depleted sample (see Sect. 2) provides a check on the light quark background. The means and widths of the B-depleted impact parameter, decay distance and dipole moment distributions are reproduced by the Monte Carlo within statistical errors.

The Lund Monte Carlo model has been used to examine the relative contribution of the light quark background. Efficiencies for selecting $u\bar{u}, d\bar{d}$, $s\bar{s}$ and $c\bar{c}$ events, vertices and tracks as well as the average impact parameter, decay distance and dipole moment for each flavor agree with the QCDFF Monte Carlo simulation to within 10%. There is a tendency for Lund to predict a slightly higher background, suggesting a slightly longer B lifetime. Replacement of the light quark events by those from Lund results in an increase in the measured B lifetime of 8–13%.

If the model of the fragmentation process is incorrect, this may be evident as a smooth variation of the measured lifetime with the value of a track moment cut. These cuts for all methods have been varied over wide ranges. No such trends are observed and fluctuations in the measured lifetimes are below 10%. Different schemes for weighting the vertices in the Vertex Method and the tracks in the dipole method have been tried, including uniform weighting. No significant changes are seen.

Another check is the effect of the cuts to suppress three-jet events. The analyses have been repeated with different cuts and the measured values are unchanged within 5%.

The transverse fragmentation parameter, σ_q, has also been varied by ±10% in both the QCDFF and the Lund Monte Carlo simulations. The resulting variations in the measured lifetimes are less than 7%. For the dipole method, the other parameters fitted in the QCDFF model, i.e. the strong coupling constant α_s and the light quark fragmentation parameter α_F, were individually varied by ±10%. The measured lifetime changed by not more than 9%. A similar range of parameters in the Lund model, using both Peterson and symmetric charm quark fragmentation, produced a similar variation in measured lifetime.

These checks are used to put upper limits on the uncertainty in the flavor fractions. These limits correspond to 15–25% in overall efficiency for $b\bar{b}$ and $c\bar{c}$ contributions and give rise to conservative systematic error estimates of $\delta\tau_B = \pm 0.22$ (IP), $^{+0.18}_{-0.15}$ (VX) and $^{+0.20}_{-0.15}$ (DM) ps for the three methods. These limits are asymmetric for two of the methods since some

of these checks, notably the use of the Lund Monte Carlo model lead predominantly to increases in the measured lifetime.

Adding the contributions discussed so far in quadrature, systematic errors of $\delta\tau_B = \pm 0.25$ (IP), ± 0.24 (VX) and ± 0.25 (DM) ps are estimated due to uncertainties in the modelling of hadronic events.

6.5 *Detector effects*

Effects of the detector have been studied extensively and a very detailed simulation of the vertex detector has been implemented. This simulation includes non-Gaussian and drift time-dependent resolution tuned to hadronic data, and a complete noise simulation obtained by superimposing an individual real random trigger event on each generated event.

The influence of the beam spot position has been checked by shifting it in the x and y directions by 100 μm. The size of the beam spot has also been varied by $\pm 20\%$. We have checked for variations with the point resolution of the VXD, the number of hits recorded per track in the VXD and the overall impact parameter resolution. In addition we have checked for uniformity of our results under translation and rotation of the VXD and for uniformity among subsamples of events whose sphericity axes lie in different azimuthal ranges. These effects are all found to be negligible. As noted above, the widths of the distributions for B-depleted samples are in good agreement with the Monte Carlo simulation.

The impact parameter and dipole methods are sensitive to a systematic shift in the measured mean of the impact parameter distribution. Studies of the residuals of track hits in the VXD and of the B-depleted sample limit any such shift to less than 3 μm. This corresponds to errors of $\delta\tau_B = \pm 0.05$ (IP) and ± 0.15 (DM) ps on these two methods. Also the impact parameter method is sensitive to the value of the cut used to reject spurious tracks with large impact parameter. This contributes a systematic error of $\delta\tau_B = \pm 0.10$ (IP) ps.

The vertex method is quite sensitive to the resolution on the measured decay distance as this directly affects the fit. This resolution is varied in both directions until the binned χ^2 on the negative side of the decay distance distribution is doubled. This gives a change in the measured lifetime of $\delta\tau_B = \pm 0.09$ (VX) ps.

The accuracy of the sphericity axis as a measure of the B hadron flight direction(s) is also important. This is dominated by the accuracy of the sphericity axis as a measure of the true jet direction. The average angle between the axis and the flight direction is varied in the Monte Carlo simulation by $\pm 20\%$, giving estimated errors of $\delta\tau_B = \pm 0.05$ (IP), ± 0.05 (VX) and ± 0.03 (DM) ps.

Table 2. Summary of systematic errors on τ_B. All entries in ps

Error source	Impact parameter	Vertex	Dipole	Combined
b Fragmentation	$+0.09$	$+0.13$ -0.15	± 0.11	± 0.12
c Fragmentation	± 0.04	± 0.06	± 0.05	± 0.05
Charm lifetime	± 0.05	± 0.09	± 0.08	± 0.08
B decay multiplicity	± 0.05	± 0.05	± 0.06	± 0.05
Flavor fractions	± 0.22	$+0.19$ -0.16	$+0.20$ -0.15	± 0.16
Impact parameter shift	± 0.05	–	± 0.15	± 0.05
Impact parameter cut	± 0.10	–	–	± 0.04
Decay distance resolution	–	± 0.09	–	± 0.04
Sphericity axis	± 0.05	± 0.05	± 0.03	± 0.05
Total	± 0.28	± 0.28	± 0.30	± 0.24

6.6 *Total systematic errors*

The sources of systematic error discussed here are summarized in Table 2. Combining these in quadrature, total systematic errors of $\delta\tau_B = \pm 0.28$ (IP), ± 0.28 (VX) and ± 0.30 (DM) ps are estimated for the impact parameter, vertex and dipole methods respectively.

7 Conclusions

Three different methods have been used to measure the average lifetime of B hadrons at TASSO. The results of the three measurements are:

Impact parameter method	$\tau_B = 1.36 \pm 0.13$ (stat) ± 0.28 (syst) ps
Vertex method	$\tau_B = 1.30 \pm 0.10$ (stat) ± 0.28 (syst) ps
Dipole method	$\tau_B = 1.47 \pm 0.14$ (stat) ± 0.30 (syst) ps

These results are in good agreement with each other, with our previous measurement [7] and with published results from other collaborations [5, 6]. Our three results can be combined using a best linear unbiased estimate [24] which takes into account correlations between the three measurements due to overlapping data samples and common systematics. The majority of the systematic errors are due to parameters of the model and are therefore fully positively correlated. We take all the errors listed in Table 2 to be fully correlated with the exception of that due to fla-

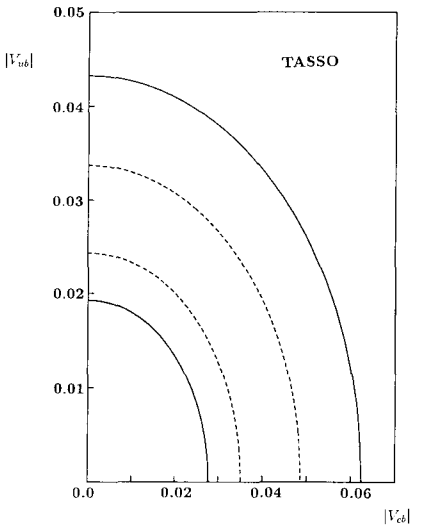

Fig. 9. Excluded range of the two Kobayashi-Maskawa matrix elements V_{ub} and V_{cb}. The region outside the two solid lines is excluded at 90% confidence by this measurement as discussed in the text. The dotted lines show this region if only the error on this lifetime measurement is considered

vor fractions. Our studies indicate that there is considerable independence here so we take this to be 50% positively correlated. The calculation is now insensitive to the statistical correlation as long as it is not too close to 1. Since the event samples selected by the different methods do not overlap considerably, this should be a good assumption. The combined result is

$$\tau_B = 1.35 \pm 0.10\,(\text{statistical}) \pm 0.24\,(\text{systematic})\ \text{ps}.$$

This measurement may be used to put constraints on the magnitudes of two Kobayashi-Maskawa matrix elements, $|V_{ub}|$ and $|V_{cb}|$. Using the relation

$$\tau_B = \frac{192\,\pi^3}{G_F^2\, m_b^5}\,\text{BR}(B \to l\nu X)\,\frac{1}{|V_{ub}|^2 + 0.48\,|V_{cb}|^2} \qquad (8)$$

with B semi-leptonic branching ratio $11.4 \pm 0.5\%$ and b quark mass 5.0 ± 0.25 GeV/c^2 [21] we exclude the region outside the band between the solid lines in Fig. 9 at 90% confidence. The width of this band is dominated by the uncertainty in the b quark mass. If this uncertainty is neglected, the region outside the two dotted lines is excluded. The ARGUS and CLEO collaborations have determined upper limits for the ratio $|V_{ub}|/|V_{cb}|$ of 0.16 [25] at 90% confidence. Taking $|V_{ub}| = 0$, we obtain $|V_{cb}| = 0.040\,^{+0.005+0.008}_{-0.003-0.005}$, where the first error is from this B lifetime measurement and includes statistical and systematic errors added in quadrature, and the second is due to uncertainties in the b quark mass and the B hadron semi-leptonic branching ratio. This measurement is unchanged for $|V_{ub}| \leqq 0.16\,|V_{cb}|$.

Table 3. Summary table of B lifetime measurements

Experiment	$b\bar{b}$ event enrichment	Quantity measured	Results (10^{-12} s)
DELCO [5]	High $p_\perp$ lepton	Lepton impact parameter	$1.17\,^{+0.27+0.17}_{-0.22-0.16}$
HRS [5]	High $p_\perp$ lepton	Lepton impact parameter	$1.02\,^{+0.41}_{-0.37}$
JADE [5]	High $p_\perp$ lepton	Lepton impact parameter	$1.80\,^{+0.50}_{-0.40} \pm 0.4$
MARK II [5]	High $p_\perp$ lepton	Lepton impact parameter	$0.98 \pm 0.12 \pm 0.13$
MAC [6]	High $p_\perp$ lepton	Hadron impact parameter	$1.29 \pm 0.20 \pm 0.21$
TASSO	Boosted sphericity product	Hadron impact parameter	$1.36 \pm 0.13 \pm 0.26$
JADE [26]	Boosted sphericity product	Distance between two decay vertices	$1.46\,^{+0.22}_{-0.21} \pm 0.34$
TASSO	None	Dipole moment	$1.47 \pm 0.14 \pm 0.30$
TASSO	None	Distance to decay vertex	$1.30 \pm 0.10 \pm 0.27$

Table 3 summarizes the most recent results from those experiments which have reported B lifetime measurements. They are classified by the methods of $b\bar{b}$ event selection and of lifetime measurement. It can be seen that agreement among the various results is quite good, even considering that there may be sizeable systematic errors common to measurements using similar methods.

In addition to the three methods presented in this paper we used data taken in 1986 at $\sqrt{s} = 35$ GeV to determine the B lifetime from semileptonic b quark decays by tagging high transverse momentum muons [27]. Applying the impact parameter method to the muon tracks we obtain $\tau_B = (1.32 \pm 0.45 \pm 0.14)$ ps, in good agreement with the result from our other methods. Because of the much bigger statistical error we do not include this in our final result on the B lifetime but regard it as a valuable check.

It is interesting to note that our B lifetime is larger by about one standard deviation than those measurements using only high transverse momentum leptons

[5]. If there is any difference between the lifetimes of the different B hadron species, then those measurements are expected to be above the true average, since the species are selected in proportion to their respective semi-leptonic branching ratios. These are expected to be proportional to their lifetimes, assuming spectator model dominance of semi-leptonic decays. We would expect to measure a lifetime no larger than the true average since our methods are slightly more sensitive to higher multiplicity decay modes. A comparison of our result with those mentioned above suggests that the lifetimes of the various species of B hadron, in particular those of the B_u^- and B_d^0 which make up most of the sample, are not very different, in agreement with limits set by the CLEO collaboration [28].

Acknowledgements. We would like to thank the PETRA machine group and the DESY computer center for their support especially in obtaining and processing the large data sample in 1986. Those of us from outside DESY wish to thank the DESY directorate for their hospitality.

References

1. M. Kobayashi, T. Maskawa: Prog. Theor. Phys. 49 (1973) 652
2. JADE Coll. W. Bartel et al.: Phys. Lett. 114B (1982) 71
3. MAC Coll. E. Fernandez et al.: Phys. Rev. Lett. 51 (1983) 1022
4. MARK II Coll. N.S. Lockyer et al.: Phys. Rev. Lett. 51 (1983) 1316
5. JADE Coll. W. Bartel et al.: Z. Phys. C – Particles and Fields 31 (1986) 349; HRS Coll. J.-M. Brom et al., Phys. Lett. B 195 (1987) 301; DELCO Coll. D.E. Klem et al.: Phys. Rev. D 37 (1988) 41; MARK II Coll. SLAC-PUB-4559, submitted to Phys. Rev. Lett.
6. MAC Coll. W.W. Ash et al.: Phys. Rev. Lett. 58 (1987) 640
7. TASSO Coll. M. Althoff et al.: Phys. Lett. 149B (1984) 524
8. TASSO Coll. R. Brandelik et al.: Phys. Lett. 83B (1979) 261; Z. Phys. C – Particles and Fields (1980) 87; H. Boerner et al.: Nucl. Instrum. Methods 176 (1980) 151; D. Binnie et al.: Nucl. Inst 282 (1985) 267
9. ARGUS Coll. H. Albrecht et al.: Phys. Lett. 185B (1987) 218; CLEO Coll. C. Bebek et al.: CLNS 86/742 (1987)
10. D. Cassel, H. Kowalski: Nucl. Instrum. Methods A185 (1981) 235
11. S.L. Wu, G. Zobernig: Z. Phys. C – Particles and Fields 2 (1979) 107
12. R. Barlow: J. Comp. Phys. 72 (1987) 202
13. TASSO Coll. W. Braunschweig et al.: Z. Phys. C – Particles and Fields 39 (1988) 331
14. A.J. Campbell: Ph.D. Thesis, Imperial College, London 1983
15. D.H. Saxon: Nucl. Instrum. Methods A234 (1985) 258
16. K. Fabricius, G. Kramer, G. Schierholz, I. Schmitt: Phys. Lett. 97B (1980) 431; Z. Phys. C – Particles and Fields 11 (1983) 315
17. A. Peterson et al.: Phys. Rev. D 27 (1983) 105
18. J. Chrin: Z. Phys. C – Particles and Fields 36 (1987) 163; E. Thorndike: Ann. Rev. Nucl. Part. Sci. 35 (1985) 195
19. TASSO Coll. M. Althoff et al.: Z. Phys. C – Particles and Fields 26 (1984) 157
20. A. Ali, J. Körner, G. Kramer, J. Willrodt: Z. Phys. C – Particles and Fields 1 (1979) 203
21. B. Gittelman, S. Stone: CLNS 87/81 (1987)
22. T. Sjöstrand: Comput. Phys. Commun. 39 (1986) 347
23. D. Hitlin in Proceedings of the 1987 International Symposium on Lepton and Photon Interactions at High Energies, Hamburg, 1987, W. Bartel, R. Rückl (eds.) p. 179. Amsterdam: North Holland 1987
24. L. Lyons, D. Gibaut, P. Clifford: Nucl. Instrum. Methods A270 (1988) 110
25. ARGUS Coll. Contributed paper, XXIV International Conference on High Energy Physics, Munich, 1988; CLEO Coll. S. Berends et al.: Phys. Rev. Lett. 59 (1987) 407
26. R. Ramcke: Ph. D. Thesis, Universität Hamburg (1988)
27. M.E. Veitch: Ph. D. Thesis, Oxford University (1989)
28. CLEO Coll. A. Bean et al.: Phys. Rev. Lett. 58 (1987) 183